ISSN 1054-660X, Laser Physics, 2010, Vol. 20, No. 3, pp. 700–708.

Quantum Entanglement via Superradiance of a Bose–Einstein Condensate[1]

M. E. Taşgın[a, *], M. Ö. Oktel[b], L. You[c], and Ö. E. Müstecaplıoğlu[c, **]

[a] *Department of Physics, Koç University, 34450 Sarıyer, Istanbul, Turkey*
[b] *Department of Physics, Bilkent University, 06800 Bilkent, Ankara, Turkey*
[c] *School of Physics, Georgia Institute of Technology, Atlanta, Georgia 30332, USA*
*e-mail: metasgin@ku.edu.tr
**e-mail: omustecap@ku.edu.tr
Received October 2, 2009; published online February 2, 2010

Abstract—We adopt the coherence and built-in swap mechanism in sequential superradiance as a tool for obtaining continuous-variable (electric/magnetic fields) quantum entanglement of two counter-propagating pulses emitted from the two end-fire modes. In the first-sequence, end-fire modes are entangled with the side modes. In the second sequence, this entanglement is swapped to in between the two opposite end-fire modes. Additionally, we also examine the photon number correlations. No quantum correlations is observed in this variable.

DOI: 10.1134/S1054660X10050191

1. INTRODUCTION

Superradiance (SR), first predicted by Dicke [1] in 1954 and first experimentally demonstrated near the optical region in 1973 by Skribanowitz et al. [2], refers to the collective spontaneous emission of an ensemble of atoms. Since the phases of atoms cohere, multi-atomic ensemble displays a macroscopic dipole moment that is proportional to the number of atoms, N. This gives rise to emission intensity proportional to the square of the number of atoms, $\sim N^2$. This resembles the intensity of overlap of N identical waves, all have the same (or very close) phase. In a normal or stimulated radiator N atoms radiate independently, giving rise to intensity proportional to N. In order to be able to observe the collective radiation, pumping time must be smaller than the decoherence time (T_2) [3] of the atomic phases.

In SR, atomic coherence induces spontaneously due to the interaction of all atoms with the common radiation field; spontaneous emission field [4]. In other collective phenomenon, such that free induction, photon echo and self-induced transparency [5, 6], intensity is also proportional to N^2. The phasing between the atoms, however, is established via the coherent pumping of the atoms to the excited state.

SR occurs in many systems [7], from thermal gases of excited atoms [8] and molecules [2], quantum dots and quantum wires [9–11], to Rydberg gases [12], and molecular nanomagnets [13]. On the other hand, however, SR in an elongated Bose–Einstein condensates (BECs) [14, 15] displays peculiar features. Due to the cooperative nature of SR, condensate atoms ($\mathbf{p} = 0$) are scattered into higher momentum states collectively. And, because of the strong directionality of the end-fire mode radiation, atoms are scattered approximately to the same momentum mode. These are called side modes. Furthermore, atoms are recoiled to side modes phase consistently due to the collectivity. When a side mode is sufficiently occupied they also give rise to superradiant scattering and form new side modes. The resulting picture, Fig. 1, is a fanlike pattern of the side modes. This phenomenon, that is observed only in BEC sample [14], is called the sequential Superradiance.

After the demonstration of SR in BEC [14], serious efforts have been directed towards the study of quantum entanglement between condensed atoms and SR light pulses [16–18]. Entanglement between atoms through SR [9] is also studied. Possibility of quantum teleportation in quantum dots via SR [9] is proposed as a promising application.

Recently, SR was observed in the Kapitza–Dirac regime [19] with short pulse pump scheme. Rather than the fanlike pattern of longer pulse pump scheme [14], momentum side modes display X-shaped pattern in the Kapitza–Dirac regime. Backscattering of the side modes are observable only in the short time intervals, since energy is not conserved in the occupation of these modes. It is predicted, in this regime, that SR pulses must contain quantum entangled counter-propagating photons from the end-fire modes [20]. The origin of the quantum entanglement is the four-wave mixing of two atomic fields (forward and backward scattered side modes) with the two photonic fields (counter-propagating end-fire modes) [20]. The predicted form of interaction, containing the terms of

[1] The article is published in the original.

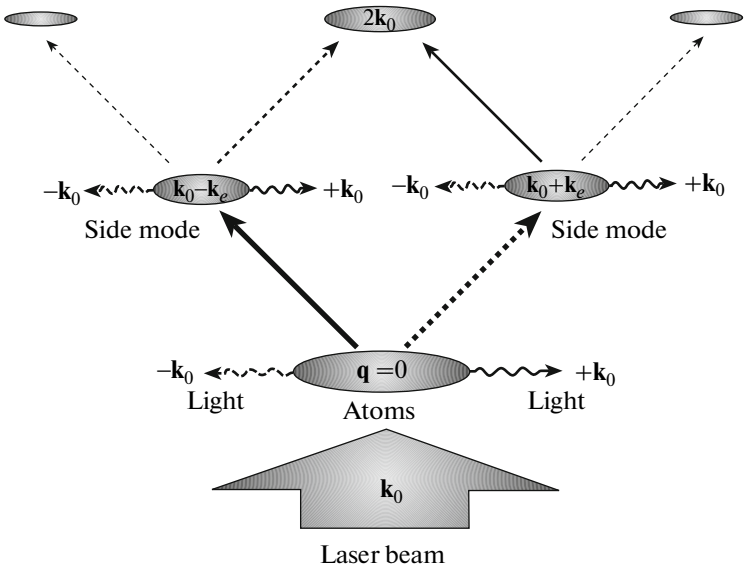

Fig. 1. (Color online) A fan-like atomic side mode pattern up to second order sequential superradiant scattering.

two-mode squeezing, suggests a continuous-variable (CV) entanglement in between the end-fire modes.

Experimental demonstration of quantum teleportation [21], via CV quantum entanglement of field amplitudes of two pulses, aroused great interest over the systems displaying CV correlations [22–25]. CV entanglement is adopted for quantum cryptology [26] as well as quantum computation [27–30]. Quantum computation is based upon the transfer of the entanglement between photon-photon, atom-atom and atom-photon pairs. The need for more durable entanglement drives the research on more correlated systems.

In this paper, we demonstrate the continuous-variable (CV) quantum entanglement of the two end-fire modes, during the sequential SR, even for a continuous-wave pumped condensate [14]. The origins of the photon-photon entanglement within the fan-like pattern, however, is quite different than the predicted one (four-wave mixing) within the X-shaped pattern [19, 20].

The atom-photon entanglement generated in the first sequence of SR is *swapped* into the photon-photon entanglement in the second sequence. This is because; the side mode interacted with the rightward-propagating end-fire mode in the first sequence, interacts with the leftward-propagating end-fire mode in the second sequence. In other words, counter-propagating end-fire modes are entangled due to the interaction with the same side mode, at. different times. In quantum information language, entanglement is swap is a technique to entangle particles that never before interacted [31–34]. We clearly identify the swapping of the entanglement in between the two pairs (atom-photon and photon-photon) in both of our analytical and computational results.

Additionally, we investigate the photon number correlation functions introduced in [35] and discussed in [36, 37]. We test the existence of quantum correlations via referring to the violation of Bell-type inequalities [38–43]. We demonstrate that the behavior of photon number correlations unparallels the CV entanglement.

The paper is organized as follows. In Section 2 we give the outline of the full second quantized effective-Hamiltonian for the present system. The details of the derivation is available in [44, 45]. CV entanglement criteria is discussed in Section 3, over which the confirmation of the existence of quantum correlations is judged. In Section 4, we solve the effective Hamiltonian analytically, under parametric and steady state approximations. We provide an intuitive argument, for the entanglement swap mechanism, to explain how such a Hamiltonian can generate EPR pairs out of non-interacting photons. In Section 5, we present our numerical results; the temporal dynamics of the entanglement and the accompanying field and atomic populations. This helps to illustrate the swapping of atom-photon entanglement to the photon-photon entanglement. In Section 6, we compare the dynamics of the correlations in the photon number with the CV entanglement. Section 7 contains our conclusions.

2. MODEL HAMILTONIAN

We consider an elongated condensate, of length L and width W, axially symmetric about the long direction of the z-axis. The pump laser with frequency ω_0 is along the y-axis and linearly polarized in the x-axis and detuned from the atomic resonance by Δ. Adiabatically eliminating the atomic excited state while keeping the pump laser quantum, not like in [46], an

effective Hamiltonian in the Fock representation is found to be

$$\hat{H} = \int d^3\mathbf{k}\hbar\omega(\mathbf{k})\hat{a}_{\mathbf{k}}^{\dagger}\hat{a}_{\mathbf{k}} + \sum_{\mathbf{q}}\hbar\omega_{\mathbf{q}}\hat{c}_{\mathbf{q}}^{\dagger}\hat{c}_{\mathbf{q}} - \frac{g(\mathbf{k}_0)}{\Delta}\sum_{\mathbf{q}\mathbf{q}'}\int d^3\mathbf{k}\rho_{\mathbf{q},\mathbf{q}'}(\mathbf{k})\hbar g^*(\mathbf{k})\hat{c}_{\mathbf{q}}^{\dagger}\hat{a}_{\mathbf{k}}^{\dagger}\hat{a}_{\mathbf{k}_0}\hat{c}_{\mathbf{q}'}, \quad (1)$$

where $\rho_{\mathbf{q},\mathbf{q}'}(\mathbf{k}) = \int d^3\mathbf{r}|\phi_0(\mathbf{r})|^2 e^{i[(\mathbf{k}+\mathbf{q})-(\mathbf{k}_0+\mathbf{q}')]\cdot\mathbf{r}}$ is the structure factor for the condensate density, $\mathbf{k}_0 = (\omega_0/c)\hat{\mathbf{y}}$, and $\phi_0(\mathbf{r})$ is unit normalized condensate wave function $\int d^3\mathbf{r}|\phi_0(\mathbf{r})|^2 = 1$. $\hat{\mathbf{y}}$ is a unit vector in the y-direction. $\hat{a}_{\mathbf{k}}$ ($\hat{a}_{\mathbf{k}}^{\dagger}$) denotes the annihilation (creation) operator for a scattered photon with wave vector $\mathbf{k}$ and frequency $\omega(\mathbf{k}) = c|\mathbf{k}| - \omega_0$. $g(\mathbf{k}) = [c|\mathbf{k}|d^2/2\hbar\epsilon_0(2\pi)^3]^{1/2}|\hat{\mathbf{k}}\times\hat{\mathbf{x}}|$ is the coefficient for atom-field coupling [17] with d the magnitude of atomic dipole moment. $\hat{c}_{\mathbf{q}}$ ($\hat{c}_{\mathbf{q}}^{\dagger}$) is the atomic side mode annihilation (creation) operator [46], and $\omega_{\mathbf{q}} = \hbar|\mathbf{q}|^2/2m$ is the side mode energy at a recoil momentum of $\mathbf{q}$.

When $L \gg W$ small angle Rayleigh scattering is negligible [15]. The angular distribution of scattered light becomes sharply peaked at the end-fire modes ($\mathbf{k}_e = \pm k_e\hat{z}$) if the Fresnel number $\mathcal{F} = W^2/L\lambda_0 \gtrsim 1$ at the pump wavelength λ_0 [46], making it possible to neglect all other scattered photon modes. We take into account the first order forward side modes at $\mathbf{q} = \mathbf{k_0} \pm \mathbf{k_e}$ and the second order side mode at $\mathbf{q} \approx 2\mathbf{k}_0$. The resulting pattern for mode coupling, depicted in Fig. 1, corresponds to what was observed for relatively long pump durations [14]. The remaining side modes are assumed unpopulated [47]. During sequential SR, the emitted photons carry approximately the same energy $\omega_0 - \omega_R$ with $\omega_R = \hbar k_0^2/2m$ being the two-photon recoil frequency, and $k_e \approx k_0$ due to energy and momentum conservations. Thus, $\omega(\mathbf{k}_e)$ is insignificant and will be neglected. The Hamiltonian (1) reduces to

$$\hat{H} = -\hbar\frac{g^2}{\Delta}(\hat{c}_+^{\dagger}\hat{a}_-^{\dagger}\hat{a}_0\hat{c}_0 + \hat{c}_-^{\dagger}\hat{a}_+^{\dagger}\hat{a}_0\hat{c}_0 + \hat{c}_2^{\dagger}\hat{a}_-^{\dagger}\hat{a}_0\hat{c}_- + \hat{c}_2^{\dagger}\hat{a}_+^{\dagger}\hat{a}_0\hat{c}_+) + \text{H.c.}, \quad (2)$$

with $g \equiv g(\mathbf{k}_e)$, where we have adopted a shorthand notation: $\hat{a}_{\pm} \equiv \hat{a}_{\pm\mathbf{k}_e}$, $\hat{a}_0 \equiv \hat{a}_{\mathbf{k}_0}$, $\hat{c}_{\pm} \equiv \hat{c}_{(\mathbf{k}_0\pm\mathbf{k}_e)}$, and $\hat{c}_2 = \hat{c}_{2\mathbf{k}_0}$.

This is the effective Hamiltonian governing the dynamics of four atomic side modes and three photonic modes. In the following sections we examine the time evolution of the entanglement parameter $\lambda(t)$ and the corresponding population dynamics under the act of this Hamiltonian. In the next section, we briefly review the CV entanglement and extend its criteria to our case.

3. CONTINUOUS-VARIABLE ENTANGLEMENT CRITERIA

If the density matrix of a quantum system is inseparable within the two modes, then the total variance of EPR-like operators, $\hat{u} = |c|\hat{x}_1 + \hat{x}_2/c$ and $\hat{v} = |c|\hat{p}_1 - \hat{p}_2/c$, satisfies the inequality $\langle\Delta\hat{u}^2\rangle + \langle\Delta\hat{v}^2\rangle < (c^2 + 1/c^2)$ [36, 48–50]. Here, $\hat{x}_{1,2} = (\hat{a}_+ + \hat{a}_+^{\dagger})/\sqrt{2}$ and $\hat{p}_{1,2} = (\hat{a}_+ - \hat{a}_+^{\dagger})/i\sqrt{2}$ are the analogous position and momentum operators, where indices corresponds to the mode numbers. c is any real number. The total variance of the operators are bounded below by the Heisenberg uncertainty relation $\langle\Delta\hat{u}^2\rangle + \langle\Delta\hat{v}^2\rangle \geq |c^2 - 1/c^2|$.

We define the inseparability parameter $\lambda(t) = \langle\Delta\hat{u}^2\rangle + \langle\Delta\hat{v}^2\rangle - (c^2 + 1/c^2)$. When the quantum state is inseparable, parameter becomes negative $\lambda(t) < 0$. Then the two modes are entangled. The value of c is fixed to the one which minimizes λ. Finding only one value of c that leads to $\lambda < 0$ is sufficient for the existence of entanglement.

Beside determining a state as being entangled, however, it is *not proven* that within two $\lambda < 0$ states, the more negative one is more entangled. Throughout the paper, we use λ as a tool only to distinguish between entangled and not entangled states, although its behavior parallels the general expectation very well.

We keep the $\langle\hat{u}\rangle^2$ and $\langle\hat{v}\rangle^2$ terms during the time evolution, unlike [36], since $\langle\hat{x}_{1,2}\rangle$ and $\langle\hat{p}_{1,2}\rangle$ do not vanish for coherent state. Parameter may as well expressed as

$$\lambda = 2(c^2\langle\hat{a}_+^{\dagger}\hat{a}_+\rangle + \langle\hat{a}_-^{\dagger}\hat{a}_-\rangle/c^2 + \text{sgn}(c)\langle\hat{a}_+\hat{a}_- + \hat{a}_+^{\dagger}\hat{a}_-^{\dagger}\rangle) - \langle\hat{u}\rangle^2 - \langle\hat{v}\rangle^2, \quad (3)$$

where $c^2 = [(\langle\hat{a}_-^{\dagger}\hat{a}_-\rangle - |\langle\hat{a}_-\rangle|^2)/(\langle\hat{a}_+^{\dagger}\hat{a}_+\rangle - |\langle\hat{a}_+\rangle|^2)]^{1/2}$ and $\hat{a}_{\pm}$ are the annihilation operators for counter-propagating end-fire modes. The sign of c is determined from the expression

$$\text{sgn}(c) = -\text{sgn}[\text{Re}\{\langle\hat{a}_+\hat{a}_-\rangle\} - \text{Re}\{\langle\hat{a}_+\rangle\}\text{Re}\{\langle\hat{a}_-\rangle\} + \text{Im}\{\langle\hat{a}_+\rangle\}\text{Im}\{\langle\hat{a}_-\rangle\}]. \quad (4)$$

We note that, atom-photon entanglement can also be tested using this criteria, by only making placements $\hat{a}_1 \longrightarrow \hat{a}_{\pm}$ and $\hat{a}_2 \longrightarrow \hat{c}_{\mp}$.

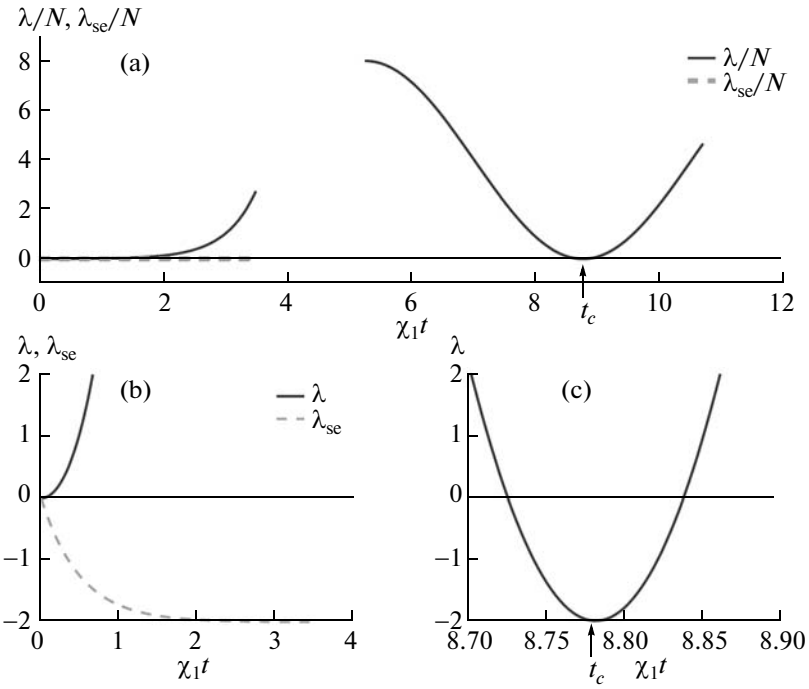

Fig. 2. The earlier and later times approximate behaviors of the entanglement parameters λ_{se} (between side mode and end-fire mode) and λ (between two end-fire modes). Atom-photon entanglement $\lambda_{se}(t)$ at initial times is swapped into photon-photon entanglement $\lambda(t)$ at later times.

The lower bound on λ is constrained by the Heisenberg uncertainty as $\lambda_{low} = |c^2 - 1/c^2| - (c^2 + 1/c^2)$. Since time evolution of the two end-fire modes are symmetric, $c^2 = 1$ and $\lambda_{low} = -2$. Thus, the correlations are over the electric/magnetic fields (**E**/**H**) of the two mode pulses (photons). When the atom-photon entanglement is to be considered, continuous-variable is the atomic (bosonic) field strength.

Throughout the paper, we examine the time evolution of the criterion parameter $\lambda(t)$, and investigate regions of negative λ for the existence of the entanglement.

4. MECHANISM OF ENTANGLEMENT SWAP

The detailed information about λ in our model system can be found by examining quantum dynamics that is based on a numerical approach as we show later. Intuitively, the generation of EPR photon pairs can be easily appreciated, based on the following argument.

Initial Times

During the initiation stage for short-time dynamics, the atom number of the condensate mode can be assumed undepleted. Taking $\hat{a}_0 = \sqrt{M}e^{i\theta_0}$ and $\hat{c}_0 = \sqrt{N}e^{i\phi_1}$, the short time dynamics is governed by

$$\hat{H}_1 = -\hbar\chi_1[e^{i\theta_1}(\hat{a}_+^\dagger\hat{c}_-^\dagger + \hat{a}_-^\dagger\hat{c}_+^\dagger) + \text{H.c.}], \qquad (5)$$

with $\chi_1 = \sqrt{NM}|g|^2/\Delta$, and $\theta_1 = \theta_0 + \phi_1$. M stands for the number of pump photons. This form of $\hat{H}_1$ is exactly the same as that of two uncoupled OPAs and, as such, allows for the growth of first-order side modes as well as their entanglement with the end-lire modes [46, 51].

We assume that all remaining quantum modes start in vacuum states. With standard solutions for $\hat{H}_1$ [5],

$$\hat{a}_\pm(t) = \cosh(\chi_1 t)\hat{a}_\pm + ie^{i\theta}\sinh(\chi_1 t)\hat{c}_\mp^\dagger, \qquad (6)$$

$$\hat{c}_\pm(t) = \cosh(\chi_1 t)\hat{c}_\pm + ie^{i\theta}\sinh(\chi_1 t)\hat{a}_\mp^\dagger, \qquad (7)$$

we can compute analytically the entanglement parameters. The operators without time arguments are at the initial time. CV entanglement parameters become

$$\lambda \equiv \lambda_{ee} = 4\sinh^2(\chi_1 t), \qquad (8)$$

$$\lambda_{se} = 2[2\sinh^2(\chi_1 t) - |\sin(\theta_1)|\sinh(2\chi_1 t)], \qquad (9)$$

where subscripts "e," "s" stand for the end-fire mode, side-mode respectively. $\lambda(t)$ shows that two end-fire modes are not entangled in the initial stage. On the other hand, end-fire modes become entangled with the oppositely scattered side modes for $|\sin\theta_1| \approx 1$, or at the pump laser phase $\theta_0 \approx \pi/2 - \phi_1$. Also, other choices of phases give entanglement but for shorter temporal periods, thus illustrating the crucial role of the relative

phase of the condensate. The initial behaviors of $\lambda(t)$ and $\lambda_{se}(t)$ are plotted in Fig. 2.

Later Times

Under conditions for sequential SR, when the second order side mode is populated at later times, rescattering dynamics is governed by

$$\hat{H}_2 = -\hbar\chi_2[e^{i\theta_2}(\hat{a}_-^\dagger\hat{c}_- + \hat{a}_+^\dagger\hat{c}_+) + \text{H.c.}], \qquad (10)$$

with $\chi_2 = \sqrt{N_2 M}|g|^2/\Delta$ and $\theta_2 = \bar{\theta}_0 + \phi_2$. Since the steady state occupation for the second order side mode $c_2 = \sqrt{N_2}e^{-i\phi_2}$ is substituted into the original Hamiltonian (2), H_2 is obviously capable of entanglement swap. The first order side mode $\mathbf{q} = \mathbf{k_0} - \mathbf{k_e}$, entangled with the end-fire mode $\mathbf{k_e}$, interacts with the counter-propagating end-fire mode $-\mathbf{k_e}$. As a result, the two end-fire modes, that never before interacted, become entangled.

To appreciate the swap mechanism in action, we use the solutions of H_1 (6, 7) as the initial state (at $t = t_0$) for dynamics due to H_2 (10). The solutions of $\hat{H}_2$ in the Heisenberg picture are

$$\hat{a}_\pm(t) = \cos(\chi_2\Delta t)\hat{a}_\pm + ie^{i\theta_2}\sin(\chi_2\Delta t)\hat{c}_\pm, \qquad (11)$$

$$\hat{c}_\pm(t) = \cos(\chi_2\Delta t)\hat{c}_\pm + ie^{-i\theta_2}\sin(\chi_2\Delta t)\hat{a}_\pm, \qquad (12)$$

where $t > t_0$, the operators without time arguments are at $t = t_0$, and $\Delta t = t - t_0$. We determine the entanglement parameters for later time to be

$$\lambda(t) = 4\sinh^2(\chi_1 t_0) - 2\left|\cos(\bar{\theta})\sin(2\chi_2\Delta t)\right|\sinh(2\chi_1 t_0), \qquad (13)$$

$$\lambda_{se}(t) = 4\sinh^2(\chi_1 t_0) - 2\left|\sin(\theta_2)\cos(2\chi_2\Delta t)\right|\sinh(2\chi_1 t_0). \qquad (14)$$

When $|\cos(\bar{\theta})| \simeq 1$, $\lambda(t)$ evolves from $2N$ down to the minimum possible negative value of $\lambda_{low} = -2$, at $\Delta t = \pi/4\chi_2$. Later dynamics of $\lambda(t)$ and $\lambda_{se}(t)$ are plotted in Fig. 2.

Thus, when H_2 acts on correlated states of end-fire modes and side modes, it is capable of swap entanglement to the counter-propagating end-fire modes.

5. RESULTS AND DISCUSSION

For a more detailed and quantitative picture, we present numerical results. The entanglement parameter λ is determined by expectation values of both operators and their products. Using the Heisenberg equation of motion, the dynamics of two operator products depend on four operator products, four operator products depend on six operator products, and so on. Such a hierarchy of operator equations is difficult to manage in general, and we will resort to a decorrelation approximation that truncates it to a closed form. The usual treatment of this sort for the SR system closes the chain too early by a simple decorrelation of atomic and optical operators, which is clearly inappropriate when entanglement swap is to be studied. We therefore adopt a decorrelation rule that factorizes condensate and the second order side mode operators in operator products, since quantum correlations between the condensate and other modes are expected to be weak due to its almost coherent-state-like nature and the second order side mode is significantly populated only at later stages of dynamics. Our approach makes it possible to keep quantum correlations between the end-fire modes and the intermediate side modes. The hierarchy of equations is closed under $\langle xyz\rangle \approx \langle xy\rangle\langle z\rangle$, with $x, y \in \{1, c_\pm, c_\pm^\dagger, a_\pm, a_\pm^\dagger\}$ and $z \in \{c_0, c_0^\dagger, c_2, c_2^\dagger\}$. These equations are solved numerically for an initial Fock state vacuum. The parameters, we used in the simulations, are as in the experiment [14].

In Fig. 3, the temporal evolution of optical field intensities and atomic side mode populations are plotted. The figure is totally symmetric with respect to $t = t_c = 0.055$ ms. The peak in the intensity after t_c is the analog of the Chiao ringing [52] in the 4-mode situation. Such a complete ringing cannot be observed in the experiments, due to the finite lifetime of the excited levels, and decoherence.

Temporal evolution of the entanglement parameters λ_{ee} (photon-photon) and λ_{se} (atom-photon) are plotted in Fig. 4, over the population dynamics, depicted in Fig. 3. The lower panel of Fig. 4 demonstrates the swap dynamics. The initial atom-photon entanglement (λ_{se}) is seen to evolve continuously into entanglement between the two end-fire modes (λ). Both of the parameters λ_{se} and λ can reach down to the lowest possible value, $\lambda_{low} = -2$, that is the Heisenberg uncertainty limit (as in the fourth section). The complete numerical results match well with the analytic solutions, depicted in Fig. 2, for the model Hamiltonians (5) at early times and (10) at later times.

We find that, in the time interval of $t = 0$–0.045 ms, the system is dominated by the 1st sequence of SR. The atomic condensate is pumped from zero-momentum state $|c_0\rangle$ initial state into the 1st order side modes $|c_\pm\rangle$. This is the reason for the overlap of $n_\pm(t)$ with $I_\pm(t)$ during this interval. Due to the interaction between the side modes and the end-fire modes, scattered into opposite directions, they become CV entangled. Thus, λ_{se} becomes negative in this region.

When the $|c_\pm\rangle$ side modes become maximally occupied at about $t = 0.045$ ms, the 1st sequence of SR is

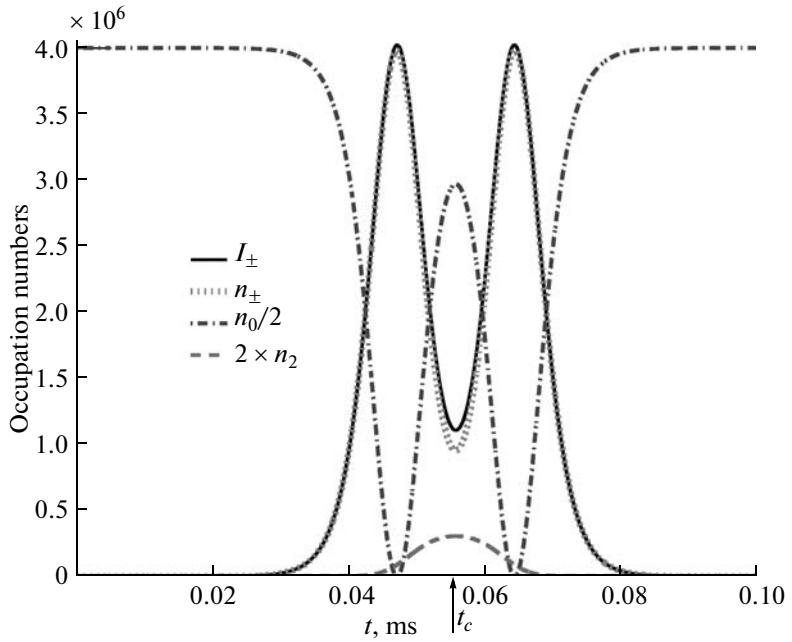

Fig. 3. The temporal evolutions for atomic side mode populations and optical field intensities. $I_\pm$, $n_\pm$, n_0, and n_2 denote occupancy numbers of bosonic modes $|a_\pm\rangle$, $|c_\pm\rangle$, $|c_0\rangle$, and $|c_2\rangle$, respectively. $n_\pm(t)$ and $I_\pm(t)$ overlap except for a short time interval near $t = t_c = 0.055$ ms. Notice that n_0 and n_2 are scaled for visual clarity.

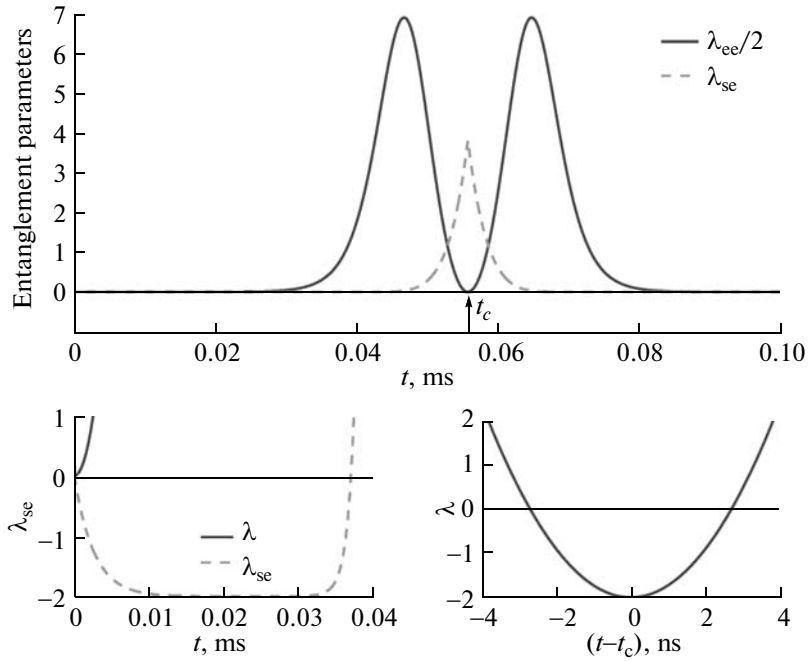

Fig. 4. (a) The temporal evolutions of atom-photon ($|a_\pm\rangle \longleftrightarrow |c_\mp\rangle$) and photon-photon ($|a_+\rangle \longleftrightarrow |a_-\rangle$) mode correlations as evidenced by the entanglement parameters λ_{se} and $\lambda \equiv \lambda_{ee}$, respectively. Accompanying population dynamics is plotted in Fig. 3. (b) An expanded view of the early time dynamics for λ_{se} and λ; (c) an expanded view of λ around $t_c = 0.055$ ms.

completed. At this time, these side modes are sufficiently populated and they give rise to the 2nd sequence of SR.

In the interval $t = 0.045$–0.055 ms atoms in the side modes $|c_\pm\rangle$ are pumped into the 2nd order side mode $|c_2\rangle$. The majority of the populations, however, oscil-

lates back to the $|c_0\rangle$ mode because of the more dominant Rabi oscillation between the $|c_0\rangle$ and $|c_\pm\rangle$ modes. Two other reasons also contribute to the repopulation of the condensate mode: first, the neglect of the propagational induced departure of the end-fire mode photons from the atomic medium; and second, the neglect of the other two 2nd order side modes $|c_{2\mathbf{k}_0 \pm 2\mathbf{k}_e}\rangle$ for atoms to get into. Two end-fire modes get indirectly coupled by the entanglement swapping and between $t = 0.045$–0.055 ms $\lambda(t)$ gradually becomes negative.

At $t = t_c = 0.055$ ms entanglement of the end-fire modes arises, when the $|c_2\rangle$ mode is maximally occupied as depicted in Fig. 4. At $t = t_c$, the minimum value of λ is found to coincide with the maximum value of $n_2(t)$.

However, due to our approximation which does not include higher side modes, when $t > t_c$ we cannot study any effects which could potentially give rise to higher order correlations, such that the onset of the 3rd sequence of SR. The oscillatory Chiao type ringing revivals in the present result after $t > t_c$ mainly arise from the exclusion of decoherence, dephasing, dissipations, and the higher order side modes in the model system. In the present work, we limited ourselves to a particular side mode pattern as actually observed in available experiments [14].

6. PHOTON NUMBER CORRELATIONS

We also investigate the photon number correlations, beside the correlations in between the electric/magnetic fields. The Bell-type inequalities exploring the quantum correlations among the photon numbers of the two modes are derived in [35, 37] as

$$B(t) = \sqrt{2}\frac{\langle \hat{a}_1^{\dagger^2}\hat{a}_1^2\rangle + \langle \hat{a}_2^{\dagger^2}\hat{a}_2^2\rangle - 4\langle \hat{a}_1^\dagger \hat{a}_2^\dagger \hat{a}_1 \hat{a}_2\rangle}{\langle \hat{a}_1^{\dagger^2}\hat{a}_1^2\rangle + \langle \hat{a}_2^{\dagger^2}\hat{a}_2^2\rangle + 2\langle \hat{a}_1^\dagger \hat{a}_2^\dagger \hat{a}_1 \hat{a}_2\rangle}. \quad (15)$$

When $|B(t)| > 2$ Bell-type inequality is violated, pointing out the existence of nonlocal correlations among the two subsystems. We evaluate $B(t)$ in the parametric and steady state approximations, discussed in the previous sections, and search for the possible photon number correlations.

Initial Times

In the initial times, the time development of the end-fire mode annihilation operators $\hat{a}_\pm(t)$ are given by Eq. (6). Inserting Eq. (6) into the expression for $B(t)$ in (15), we obtain a constant B-parameter

$$B(t) = 0, \quad (16)$$

for the earlier time development. The evaluated second order moments are

$$\langle \hat{a}_\pm^{\dagger^2}\hat{a}_\pm^2\rangle = 2\sinh^4(\chi_1 t), \quad (17)$$

$$\langle \hat{a}_+^\dagger \hat{a}_-^\dagger \hat{a}_+ \hat{a}_-\rangle = \sinh^4(\chi_1 t). \quad (18)$$

Later Times

In the later times, the time development of $\hat{a}_\pm(t)$ operators are obtained by substitution of (6) and (7) into (11) as

$$\begin{aligned}\hat{a}_\pm(t) &= C_1 C_2 \hat{a}_\pm + ie^{i\theta_1} S_1 C_2 \hat{c}_\mp^\dagger \\ &+ ie^{i\theta_2} C_1 S_2 \hat{c}_\pm - e^{i(\theta_1+\theta_2)} S_1 S_2 \hat{a}_\mp^\dagger,\end{aligned} \quad (19)$$

where $C_1 \equiv \cosh(\chi_1 t_0)$, $S_1 \equiv \sinh(\chi_1 t_0)$ and $C_2 \equiv \cos(\chi_2 \Delta t)$, $S_2 \equiv \sin(\chi_2 \Delta t)$ shorthand notations are adopted. Operators $\hat{a}_\pm$ and $\hat{c}_\pm$ are time independent. Substitution of calculated moments

$$\langle \hat{a}_\pm^{\dagger^2}\hat{a}_\pm^2\rangle = 2\sinh^4(\chi_1 t_0), \quad (20)$$

$$\langle \hat{a}_+^\dagger \hat{a}_-^\dagger \hat{a}_+ \hat{a}_-\rangle = S_1^4 + 4S_1^2 C_1^2 \sin^2(\chi_2 \Delta t)\cos^2(\chi_2 \Delta t) \quad (21)$$

yields the B-parameter

$$B(t) = -2\sqrt{2}\frac{(1+S_1^2)\sin^2(2\chi_2 \Delta t)}{3S_1^2 + (1+S_1)^2 \sin^2(2\chi_2 \Delta t)} \quad (22)$$

at the later stage. $\Delta = t - t_0$ is again gives the elapsed time after the second Hamiltonian $\hat{H}_2$ (10) is turned on.

The time evolution of $B(t)$, both in the initial and the later times, is plotted in the bottom panel of Fig. 5. We observe that photon number correlations never establishes; B-parameter remains in the interval $|B(t)| < 2$, which does not violate the positiveness of classical probabilities.

In Fig. 5, also the behaviors of $\lambda(t)$ and $B(t)$ are compared. The evolutions of $\lambda(t)$ and $B(t)$ are totally different, except that sign of $d^2\lambda(t)/dt^2$ traces the sign of $dB(t)/dt$ that has no physical implication. Any parallelism between $\lambda(t)$ and $B(t)$ is already not expected [36]. This is because; these two parameters refer to correlations in between different types of observables. λ judges the nonlocal correlations in between the electric/magnetic field observables of the two modes. Where as, $B(t)$ witnesses the correlations in the number of counted photons of the two modes.

The differences in between $\lambda(t)$ and $B(t)$ becomes evident and more clear if the behavior of $B(t)$ is investigated [35] under the two-mode squeezing Hamiltonian $H = \hbar(\xi^* \hat{a}_1 \hat{a}_2 + \xi \hat{a}_1^\dagger \hat{a}_2^\dagger)$. The evaluated

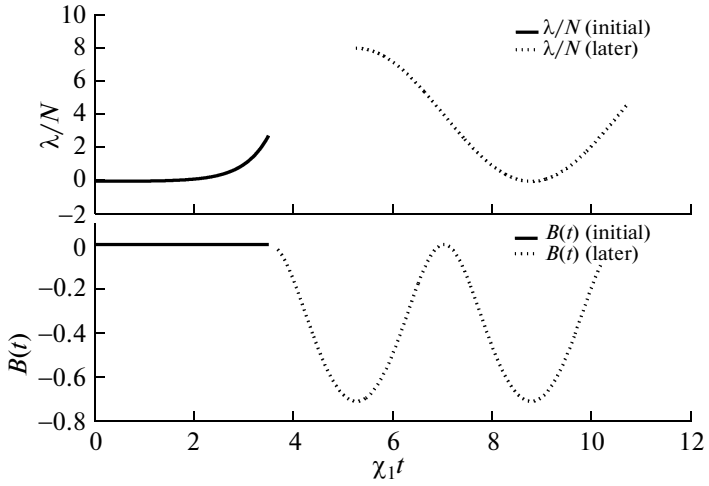

Fig. 5. The earlier and later times approximate behaviors of the entanglement parameters $\lambda(t)$ (revealing correlations in the electric/magnetic fields) compared with the $B(t)$ (revealing the photon number correlations of two modes). $B(t)$ does not exhibit violation of the Bell-type inequality, such as $|B(t)| > 2$. And, as already expected, there exists no parallelism in between $\lambda(t)$ and $B(t)$.

B-parameter, under this Hamiltonian, $B(t) = -2\sqrt{2}\dfrac{1+\sinh^2(\xi t)}{1+4\sinh^2(\xi t)}$ starts the time evolution in the photon number correlated state $B(0) = -2\sqrt{2}$, but evolves to uncorrected state within the time $1/\xi$. On the other hand however, under the same Hamiltonian and with the same initial state (Fock-state vacuum), $\lambda(t)$ starts from $\lambda(t) = 0$ (compare Eq. (14) and $\hat{H}_1$ in Eq. (5)) and evolves to the more correlated state $\lambda = -2$.

7. CONCLUSIONS

Photon–photon entanglement between the counter-propagating end-fire modes, of a sequentially superradiant atomic Bose–Einstein condensate is investigated. Atom–photon entanglement in between the oppositely scattered end-fire mode and side mode is also studied. The temporal evolution of the continuous-variable entanglement witness parameter is calculated for suitable realistic experimental parameters in the CW-pump laser regime [14]. It is shown that; EPR like correlations can be generated in between the oppositely directed end-fire modes, even though they do not interact directly.

Entanglement originates from a built-in swap mechanism: The entanglement in between end-fire mode and side mode, in the first sequence of SR, is shown to be swapped into the entanglement between the two counter-propagating end-fire modes, in the second sequence.

In addition, a Bell-type inequality governing the photon number correlations of the two end-fire modes are also studied. We observe that, Bell-type inequality is not violated for the photon number correlations.

ACKNOWLEDGMENTS

M.Ö.O. is supported by a TÜBA/GEBİP grant and TÜBİTAK-KARİYER Grant no. 104T165.

REFERENCES

1. R. H. Dicke, Phys. Rev. **93**, 99 (1954).
2. N. Skribanowitz, I. P. Herman, J. C. MacGillivray, and M. S. Feld, Phys. Rev. Lett. **30**, 309 (1973).
3. M. Sargent, M. O. Scully, and W. E. Lamb, *Laser Physics* (Addison-Wesley, Reading, MA, 1974).
4. A. V. Andreev, V. I. Emel'yanov, and Y. A. Il'inskii, *Cooperative Effects in Optics: Superradiance and Phase Transitions* (Inst. of Physics, Bristol, 1993).
5. L. Mandel and E. Wolf, *Optical Coherence and Quantum Optics* (Cambridge Univ., Cambridge, 1995).
6. M. O. Scully and M. S. Zubairy, *Quantum Optics* (Cambridge Univ., Cambridge, 1997).
7. M. Gross and S. Haroche, Phys. Rep. **93**, 301 (1982).
8. Q. H. F. Vrehen, H. M. J. Hikspoors, and H. M. Gibbs, Phys. Rev. Lett. **38**, 764 (1977).
9. j Y. N. Chen, D. S. Chuu, and T. Brandes, Phys. Rev. Lett. **90**, 166802 (2003).
10. Y. N. Chen, C. M. Li, D. S. Chuu, and T. Brandes, New J. Phys. **7**, 172 (2005).
11. A. Mitra, R. Vyas, and D. Erenso, Phys. Rev. A **76**, 052317 (2007).
12. T. Wang, S. F. Yelin, R. Côté, E. E. Eyler, S. M. Farooqi, P. L. Gould, M. Koštrun, D. Tong, and D. Vrinceanu, Phys, Rev. A **75**, 033802 (2007).
13. V. I. Yukalov, Laser Phys. **12**, 1089 (2002); V. I. Yukalov, and E. P. Yukalova, Laser Phys. Lett. **2**, 302 (2005); V. I. Yukalov, Phys. Rev. B **71**, 184432 (2005); V. I. Yukalov, Laser Phys. Lett. **2**, 356 (2005); V. I. Yukalov, V. K. Henner, and P. V. Kharebov, Phys. Rev. B **77**, 134427 (2008); V. I. Yukalov, V. K. Henner, P. V. Kharebov, and E. P. Yukalova, Laser Phys. Lett. **5**, 887 (2008).

14. S. Inouye, A. P. Chikkatur, D. M. Stamper-Kurn, J. Stenger, D. E. Pritchard, and W. Ketterle, Science **285**, 571 (1999).
15. O. E. Mustecaplioglu and L. You, Phys. Rev. A **62**, 063615 (2000).
16. M. G. Moore and P. Meystre, Phys. Rev. Lett. **85**, 5026 (2000).
17. M. G. Moore, O. Zobay, and P. Meystre, Phys. Rev. A **60**, 1491 (1999).
18. M. G. Moore and P. Meystre, Phys. Rev. A **59**, R1754 (1999).
19. D. Schneble, Y. Torii, M. Boyd, E. W. Streed, D. E. Pritchard, and W. Ketterle, Science **300**, 475 (2003).
20. H. Pu, W. Zhang, and P. Meystre, Phys. Rev. Lett. **91**, 150407 (2003).
21. A. Furusawa, J. L. Sorensen, S. L. Braunstein, C. A. Fuchs, H. J. Kimble, and E. S. Polzik, Science **282**, 706 (1998).
22. S. L. Braunstein and P. van Loock, Rev. Mod. Phys. **77**, 513 (2005).
23. G. Adesso and F. Illuminati, J. Phys. A: Math. Theor. **40**, 7821 (2007); G. Adesso and F. Illuminati, New J. Phys. **8**, 15 (2006).
24. E. G. Cavalcanti, C. J. Foster, M. D. Reid, and P. D. Drummond, Phys. Rev. Lett. **99**, 210405 (2007); A. Salles, D. Cavalcanti, and A. Acin, Phys. Rev. Lett. **101**, 040404 (2008); Q. Sun, H. Nha, and M. S. Zubairy, Phys. Rev. A **80**, 020101(R) (2009).
25. L. Praxmeyer, B.-G. Englert, and K. Wodkiewicz, Eur. Phys. J. D **32**, 227 (2005); L. Zhang, A. B. Uren, R. Erdmann, K. A. ODonnell, C. Silberhorn, K. Banaszek, and I. A. Walmsley, J. Mod. Opt. **54**, 707 (2007); Y.-X. Ping and Z. Cheng, Chin. Phys. Lett. **24**, 609 (2007). 26. A. K. Ekert, Phys. Rev. Lett. **67**, 661 (1991).
27. A. Barenco, D. Deutsch, and A. Ekert, Phys. Rev. Lett. **74**, 4083 (1995).
28. S. L. Braunstein, Nature **394**, 47 (1998).
29. S. Lloyd, Phys. Rev. Lett. **82**, 1784 (1999).
30. A. S. Parkins, and H. J. Kimble, J. Opt. B: Quantum Semiclass. Opt. **1**, 496 (1999).
31. M. Żukowski, A. Zeilinger, M. A. Horne, and A. K. Ekert, Phys. Rev. Lett. **71**, 4287 (1993).
32. C. H. Bennett, G. Brassard, C. Crépeau, R. Jozsa, A. Peres, and W. K. Wootters, Phys. Rev. Lett. **70**, 1895 (1993).
33. S. Bose, V. Vedral, and P. L. Knight, Phys. Rev. A **57**, 822 (1998).
34. J.-W. Pan, D. Bouwmeester, H. Weinfurter, and A. Zeilinger, Phys. Rev. Lett. **80**, 3891 (1998).
35. M. D. Reid and D. F. Walls, Phys. Rev. A **34**, 1260 (1986).
36. Y. Ping, B. Zhang, Z. Cheng, and Y. Zhang, Phys. Lett. A **362**, 128 (2007).
37. N. A. Ansari, Phys. Rev. A **55**, 1639 (1997).
38. J. S. Bell, Physics **1**, 195 (1965).
39. J. S. Bell, *Foundation of Quantum Mechanics*, Ed. by B. d'Espagnat (Academic, New York, 1971), p. 171.
40. A. Einstein, B. Podolsky, and N. Rosen, Phys. Rev. **47**, 777 (1935).
41. W. J. Munro, K. Nemoto and A. G. White, quant-ph/0102119v2 (2001).
42. R. F. Werner and M. M. Wolf, quant-ph/0107093v2 (2001).
43. G. Gour, F. C. Khanna, A. Mann, and M. Revzen, quant-ph/0308063v2 (2003).
44. M. E. Taşgin, M. Ö. Oktel, L. You, and Ö. E. Müstecaphoğlu, Phys. Rev. A **79**, 053603 (2009).
45. M. E. Taşgin, *Quantum Entanglement and Light Propagation through a Bose–Einstein Condensate*, PhD Dissertation (Bilkent Univ., 2009).
46. M. G. Moore and P. Meystre, Phys. Rev. Lett. **83**, 5202 (1999).
47. O. Zobay and G. M. Nikolopoulos, Phys. Rev. A **73**, 013620 (2006).
48. L. M. Duan, G. Giedke, J. I. Cirac, and P. Zoller, Phys. Rev. Lett. **84**, 2722 (2000).
49. A. Peres, Phys. Rev. Lett. **77**, 1413 (1996).
50. R. F. Werner, Phys. Rev. A **40**, 4277 (1989).
51. M. G. A. Paris, M. Cola, N. Piovella, and R. Bonifacio, Opt. Commun. **227**, 349 (2003).
52. D. C. Burnham, and R. Y. Chiao, Phys. Rev. **188**, 667 (1969).